

November seesaw in northern extratropical sea level pressure and its linkage to the preceding wintertime Arctic Oscillation

Yeon-Woo Choi,^a Joong-Bae Ahn^{a*} and Vladimir N. Kryjov^b

^a Division of Earth Environmental System, Pusan National University, Busan, Republic of Korea

^b APEC Climate Center, Busan, Republic of Korea

ABSTRACT: This paper examines the impact of the wintertime Arctic Oscillation (AO) on the following November circulation. The application of a set of statistical methods shows that a response of November sea level pressure (SLP) to the preceding wintertime AO operates on a hemispheric scale. At high and middle latitudes, this response is a well-pronounced seesaw in SLP between the Eastern and Western Hemispheres. Winters of the positive AO polarity tend to be followed by positive SLP anomalies spanning the whole Northern Eurasia and negative SLP anomalies extending from the Bering Sea through the Western North Atlantic. Opposite SLP anomalies prevail after winters of the negative AO polarity. The response of November SLP to the preceding wintertime AO closely resembles the first empirical orthogonal function of November SLP. That is, the polarity of the wintertime AO precedes the polarity of the leading mode of variability of November SLP over the Northern Hemisphere. The wintertime AO exerts a 9-month lag impact on November circulation due to the re-emergence of a sea surface temperature anomaly over the western North Atlantic.

KEY WORDS wintertime AO; November seesaw mode; SST anomaly re-emergence

Received 21 October 2014; Revised 12 April 2015; Accepted 4 June 2015

1. Introduction

The Arctic Oscillation (AO), recognized by Thompson and Wallace (1998), is a dominant mode of the wintertime climate variability in the Northern Hemisphere. Interest in the AO and in its potential effects on mid- and high-latitude climate in the Northern Hemisphere has been increasing. Many studies have reported concurrent relationships between wintertime climate variables and the AO (Thompson and Wallace, 2000; Thompson *et al.*, 2000; Gong *et al.*, 2001), while others have demonstrated that the wintertime AO significantly affects climate variables in the following months, with a memory of the wintertime AO being kept by surface persistent anomalies, particularly snow cover on the land (e.g. Kryjov, 2002; Bamzai, 2003; Ogi *et al.*, 2003a, 2003b, 2004a, 2004b; Barriopedro *et al.*, 2006), sea ice in the Nordic seas (e.g. Rigor *et al.*, 2002; Wu *et al.*, 2006) and sea surface temperature (SST; e.g. Kryjov, 2002; Ogi *et al.*, 2003a, 2003b).

Kryjov (2004) and Kryzhov (2008) have shown that November air temperature over Northeastern Europe is affected by the preceding wintertime AO due to its impact on November circulation in the Atlantic-European sector of the middle latitudes. They show that the positive (negative) wintertime AO polarity tends to be followed by a dipole anomaly in November sea level pressure (SLP) over the North Atlantic, with a negative (positive) pole over the

Labrador Sea and a positive (negative) pole over Scandinavia. These SLP anomalies lead to negative (positive) air temperature anomalies over the Northeastern Europe. This mechanism explains an observed negative trend in November temperature over this region in the 1970s–1990s, which surprisingly contrasted to the positive trend in the wintertime AO index and associated positive trend in wintertime and annual temperature (Thompson *et al.*, 2000). The negative trend in the wintertime AO index and Northeastern Europe air temperature after the 1990s is also contrasted by the positive trend in November temperature over this region. However, the studies of Kryjov (2004) and Kryzhov (2008) were confined to the Atlantic-European sector, were focused on air temperature rather than circulation and did not analyse the mechanisms of the 9-month lag in a November circulation response to the preceding wintertime AO.

This study is focused on filling the research gaps of the previous studies. We analyse the hemispheric-scale response of November circulation to the preceding wintertime AO and its consistency with the leading modes of the November SLP variability.

The most intriguing peculiarity of the November response to the polarity of the preceding wintertime AO is its occurrence after 9 months, which suggests that it cannot be explained with simple persistence of a forcing exciting it. Particularly, it cannot be explained by a persistence of the wintertime SST anomaly through November or a persistence of the anomalies of other surface properties originating in winter and persisting through the rest of the

* Correspondence to: J.-B. Ahn, Division of Earth Environmental System, Pusan National University, Jangjeon 2-dong, Geumjeong-gu, Busan 609-735, Republic of Korea. E-mail: jbahn@pusan.ac.kr

year. Explanation of the 9-month lag of the circulation response to the wintertime AO requires an environmental anomaly which is formed under the impact of the wintertime AO and reoccurs in the following autumn as a forcing affecting November circulation. Another research challenge is the timing of the significant response that is restricted to November and is not markedly noticeable in October or December. The 9-month lag and the restricted timing of the response suggest that that forcing should be a short-term 'reminder' rather than a long-living and steadily decaying 'memory'.

The role of a reminder may be played by the autumn re-emergence of the wintertime SST anomalies discussed by Alexander and Deser (1995) and Alexander *et al.* (1999). The concept of the autumn re-emergence of the wintertime SST anomalies is traced back to the works of Namias and Born (1970, 1974) and Wallace and Jiang (1987) and has been developed in the works of Alexander and Deser (1995) and Alexander *et al.* (1999). The dynamical atmospheric impact on the ocean is strong owing to wintertime storms, and the quasi-homogeneous mixed layer is very thick concurrently. Accordingly, the surface temperature anomalies formed in winter span a large depth of water. In summer, dynamical impact is much weakened, and a shallow surface quasi-homogeneous mixed layer of warm water is formed due to enhanced solar irradiance, and wintertime anomalies sink below this thin surface mixed layer, being separated from it by a thermocline. In turn, the surface warm layer is destroyed by autumn storms and preceding wintertime anomalies emerge to the surface, with the autumn SST anomalies resembling the preceding wintertime SST anomalies.

Sea ice extent anomalies that are formed in winter under the impact of the AO and persist until the autumn sea ice freezing may also act as a reminder, thereby strongly affecting autumn air temperature during freezing (Rigor *et al.*, 2002). However, a strong trend in the sea ice extent of the recent decades, exceeding its interannual variability, significantly decreases the reliability of the assessments of the interannual variability of impacts forced by sea ice anomalies, so we do not consider it in this paper.

In Section 2, we describe the primary data set and study methods. The relationships between November circulation anomalies over the Northern Hemisphere and preceding wintertime AO are studied in Section 3. Possible mechanisms of the lag response are discussed in Section 4. The conclusions are presented in Section 5.

2. Data and methods

The study was mainly performed based on the monthly mean SLP fields meshed on a $2.5^\circ \times 2.5^\circ$ grid from National Centers for Environmental Prediction/National Center for Atmospheric Research (NCEP/NCAR) Reanalysis-1 for the period 1958–2011 (Kalnay *et al.*, 1996). The studied region covers the Northern Hemisphere extratropics north of 20°N .

The monthly mean indices of the AO (Thompson and Wallace, 1998, 2000) are those of the Climate Prediction

Center (CPC), available from the CPC website. In the study, we use the January and February AO indices because the midwinter AO features the strongest interannual variability and the midwinter indices characterize the strongest impact by the AO on the environmental variables. The January–February (JF) mean AO indices were estimated as an average of January and February values.

A part of the study covers 44 years (1958–2001) because of limited availability of reliable data. Particularly, we use precipitation data from the European Centre for Medium-Range Weather Forecasts 40-year (ERA40) monthly mean reanalysis dataset (Uppala *et al.*, 2005). The zonal wind at 200 hpa data from NCEP/NCAR Reanalysis-1 are for the same period to provide consistency.

For long records of SST, we used the Centennial *in situ* Observation Based Estimates of SST version 2 (COBE-SST2) with $1^\circ \times 1^\circ$ horizontal resolution for the period 1958–2011, developed at the Japanese Meteorological Agency (Hirahara *et al.*, 2014). The subsurface temperature data used in this study are the products of the European Centre for Medium-Range Weather Forecasts (ECMWF) ocean reanalysis system 4 (ORAS4), which provides a continuous record of the global subsurface temperature by combining a wealth of observational information (Balmaseda *et al.*, 2013b). These ocean analysis data are widely used for climate analyses (e.g. Rayner *et al.*, 2009; Yasunaka and Hanawa, 2011). However, the uncertainty needs to be considered since ocean data sets consisting of gridded variables for the global ocean are based on a combination of observations that are irregularly distributed and spatially sparse. We confine our oceanic data analysis to only the North Atlantic and North Pacific because Carton *et al.* (2000) and Deser *et al.* (2010) showed that these are the areas of the highest coverage with observation since the late 1950s when an Oceanic Weather Station network was established. It has been reported that the COBE-SST data correspond well with another SST analysis based on *in situ* SST, sea ice concentration and satellite observations, especially in the Northern Hemisphere (Ishii *et al.*, 2005; Hirahara *et al.*, 2014). Balmaseda *et al.* (2013a, 2013b) argues that the reduced uncertainty in ORAS4 relative to earlier ocean reanalysis arise from the use of improved surface forcing, quality control *in situ* observation data and data assimilation method.

In order to confirm our oceanic data analysis, we used other available data sets such as the Hadley Centre sea-Ice and Sea Surface Temperature (HadISST; for the period 1958–2011; Rayner *et al.*, 2003), the Extended Reconstruction of global SST version 2 (ERSST v2; for the period 1958–2008; Smith and Reynolds, 2004), the Geophysical Fluid Dynamics Laboratory (GFDL) Ensemble Coupled Data Assimilation version 3.1 (ECDA v3.1; for the period 1961–2010; Chang *et al.*, 2013) and the Simple Ocean Data Assimilation (SODA v2.2.4; for the period 1958–2010; Carton and Giese, 2008).

We made extensive use of linear methods in our study. Correlation analysis was performed on the time series with removed linear trends. The statistical significance of the

correlation coefficients (r) was assessed by using Student's t -statistic accounting for the effective number of degrees of freedom (Bretherton *et al.*, 1999). The significance of the correlation maps was assessed by field significance tests based on the Monte-Carlo approach (Livezey and Chen, 1983), similar to that used by Kryjov (2004). Similarly to Thompson and Wallace (2000), we estimated circulation indices (CI) for the correlation maps by projecting SLP anomalies weighted by the cosine of latitude onto the correlation patterns. Therefore, each yearly CI value is proportional to a spatial regression coefficient between the correlation pattern and the corresponding SLP anomaly field. Time series of the CI were normalized.

Maximum covariance analysis (MCA) on the basis of singular value decomposition (SVD) was applied to detect coupled modes of variability of the wintertime (JF) and November SLP fields. Details of that method are described by Bretherton *et al.* (1992). The significance of the results was assessed by using the Monte-Carlo method described by Venegas *et al.* (1997). The leading modes of November SLP variability over Northern Hemisphere north of 20°N were defined by principal component analysis (PCA). Separation of the modes was assessed with the rule of thumb (North *et al.*, 1982).

3. Results

3.1. Regression analysis

A pattern of November mean SLP anomalies regressed upon the normalized JF AO index is shown in Figure 1(a). Within the polar cap north of 40°N, the pattern exhibits a marked seesaw between the Eastern and Western Hemispheres. Positive SLP anomalies span the whole North Eurasia with the largest anomalies being located over North Europe. Meanwhile, the Western Hemisphere from the Bering Sea through the western North Atlantic features remarkably negative SLP anomalies.

The regression coefficients exceed the 95% confidence threshold over the northwestern North Atlantic (negative correlations), North Europe and northern East Asia (positive correlations). The difference in the position of the largest anomalies in the regression map and the largest correlations in the correlation map is due to the difference in the variances of interannual variability of SLP in the Atlantic-European and Asia-Pacific sectors, with the variance in the former essentially exceeding that in the latter (figure not shown).

The regression map of the November mean SLP anomalies on the normalized JF AO index yields a hemispheric-scale seesaw in November SLP between the Eurasian and Pacific-American-Atlantic sectors. The polarity of this seesaw is influenced by the polarity of the preceding JF AO. Particularly, winters of the positive JF AO polarity tend to be followed by positive SLP anomalies spanning North Eurasia and negative SLP anomalies spanning North America from the North Pacific through the western North Atlantic. Opposite November SLP anomalies prevail after winters of the negative AO polarity.

To characterize the interannual variability of the obtained November SLP pattern, we constructed a November CI by projecting the area-weighted November SLP anomalies on the correlation pattern corresponding to the regression map shown in Figure 1(a). The November CI and the JF AO index significantly covariate during the whole period (Figure 1(c)), with the correlation coefficient being 0.49, which is significant at the 99% level of confidence and stable in time (Figure 1(d)). These results suggest that the mean JF AO significantly contributes to the spatial distribution of the November SLP anomalies. Additionally, we performed similar analysis using the monthly mean JF AO indices separately. The obtained results are remarkably similar to those shown for the mean JF AO.

The November seesaw mode bears some resemblance with the 'Dipole Anomaly' revealed by Wu *et al.* (2006) and Wang *et al.* (2009) and defined as a second empirical orthogonal function (EOF) mode of the cold season (October–March) SLP anomaly north of 70°N. That mode explained 13% of the total SLP variance, with 61% of the variance having been explained by the first mode, an AO-like pattern. Despite some resemblance, the November seesaw mode essentially differs from the Dipole Anomaly of Wu *et al.* (2006). Particularly, there is no covariability between the series of the CI and the Dipole Anomaly index of Wu *et al.* (2006), with the correlation coefficient being as negligible as -0.08 . In addition, the spatial patterns of these modes are fundamentally inconsistent.

The resulting regression maps (Figure 1(a) and (b)) demonstrate the influence of the wintertime AO on the November SLP anomalies. To confirm this result, we apply similar regression analysis through reverse succession. A map of JF SLP anomalies regressed on the following November CI yields an AO-like pattern (Figure 1(b)). Compared to the AO pattern of Thompson and Wallace (2000), the negative anomaly in the polar area and the positive anomaly over the North Atlantic are perfectly reproduced, whereas the positive anomaly over the North Pacific appears rather weak. Although this pattern bears some resemblance with the North Atlantic Oscillation (NAO), it is shifted northward with respect to the latter and the JF CI estimated based on the correlation pattern corresponding to the regression map shown in Figure 1(b) correlates with the JF AO index more strongly ($r = 0.95$) than with the JF NAO index ($r = 0.81$).

3.2. Maximum covariance analysis

To support the results from the regression analysis and to reveal coupled modes of variability of the November and JF SLP anomalies, we conducted MCA on the basis of SVD. The leading pair of coupled singular vectors is shown in Figure 2. The fraction of squared covariance associated with the leading pair is 43.5%. The correlation coefficient between the time series of the corresponding expansion coefficients, JF EC1 and November EC1 (Figure 2(c)), is 0.54.

The primary coupled mode of variability of JF SLP (Figure 2(a)) closely resembles the JF AO pattern, which

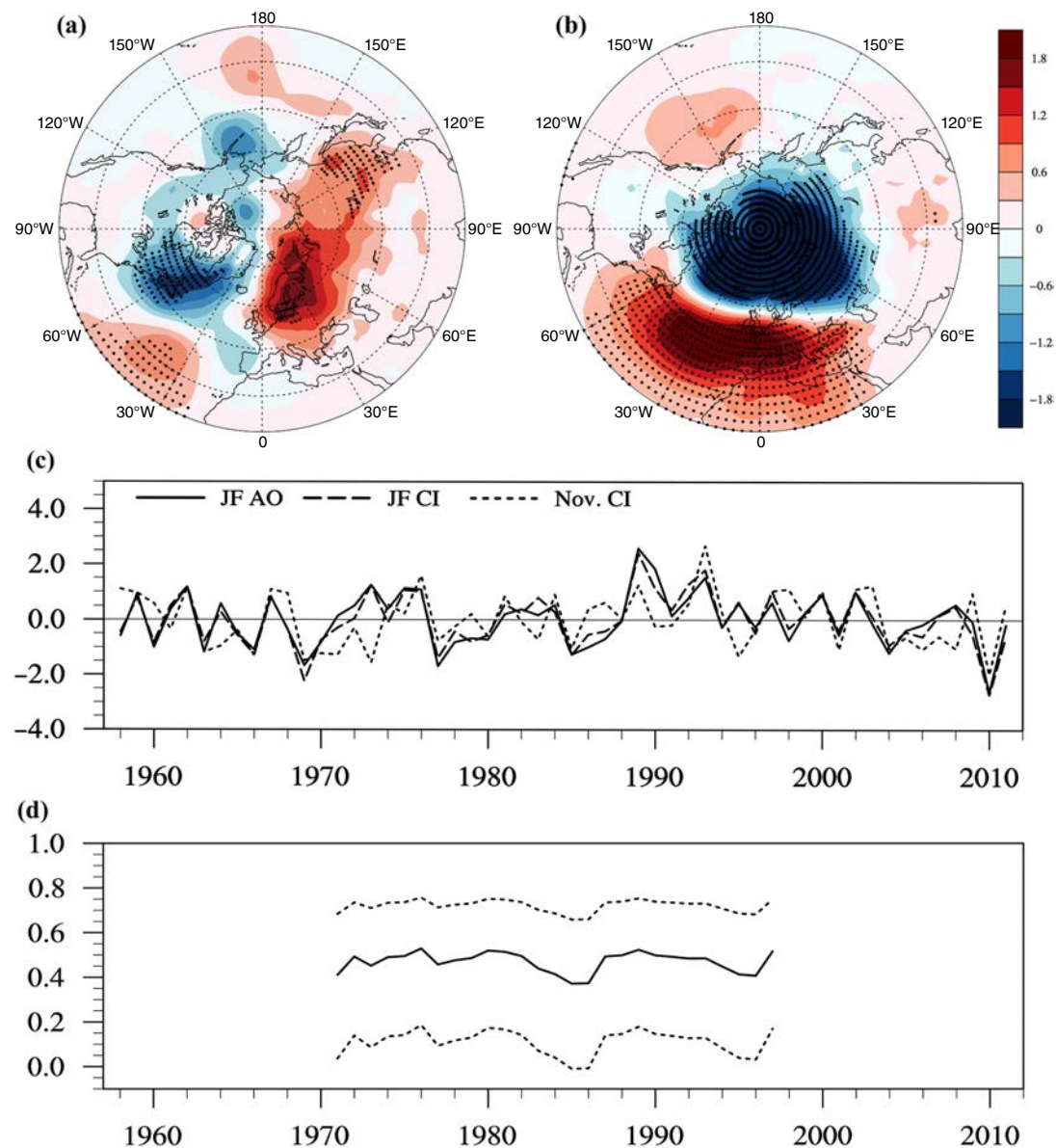


Figure 1. Regression of the November SLP anomalies on the January–February AO index (a) and regression of the January–February SLP anomalies on the November circulation index (CI) (b), unit: $\text{hPa}(\text{SD})^{-1}$; normalized time series of the JF AO, JF CI and November CI (c); running correlations calculated over 27-year windows (plotted in the central year of the 27-year period) between the January–February AO index and November CI (solid) and their 95% confidence intervals (dashed) (d). The dots in (a) and (b) indicate the area where regression coefficients are significant at the 95% confidence level.

is proved by the correlation coefficient of 0.87 between the time series of the EC1 of JF SLP and the JF AO. The leading coupled mode of variability of November SLP (Figure 2(b)) yields a hemispheric pattern with the most prominent feature being an eastern–western interhemispheric seesaw closely resembling the regression pattern shown in Figure 1(a). The correlation coefficient between the time series of the EC1 of November SLP and the November CI is 0.93.

Thus, the MCA results support the suggestion that the November SLP anomalies are influenced by the preceding wintertime AO. Particularly, both the regression and MCA analyses reveal that the positive polarity of the JF AO tends to be followed by a seesaw pattern in November SLP characterized by the positive SLP anomalies spanning

North Eurasia and negative SLP anomalies spanning the Western Hemisphere from the Bering Sea through the western North Atlantic. In Novembers following winters of the negative AO polarity, the signs of the anomalies reverse.

3.3. PCA of November SLP

In order to ascertain whether the derived November SLP response to the JF AO is a prominent pattern of the November SLP variability or is an artefact of the applied methods, we performed PCA of November SLP anomalies over the extratropical Northern Hemisphere poleward of 20°N . The first PCA mode of November SLP accounts for 19% of its total variance, is well separated from the following mode according to the rule of thumb (North *et al.*, 1982) and the

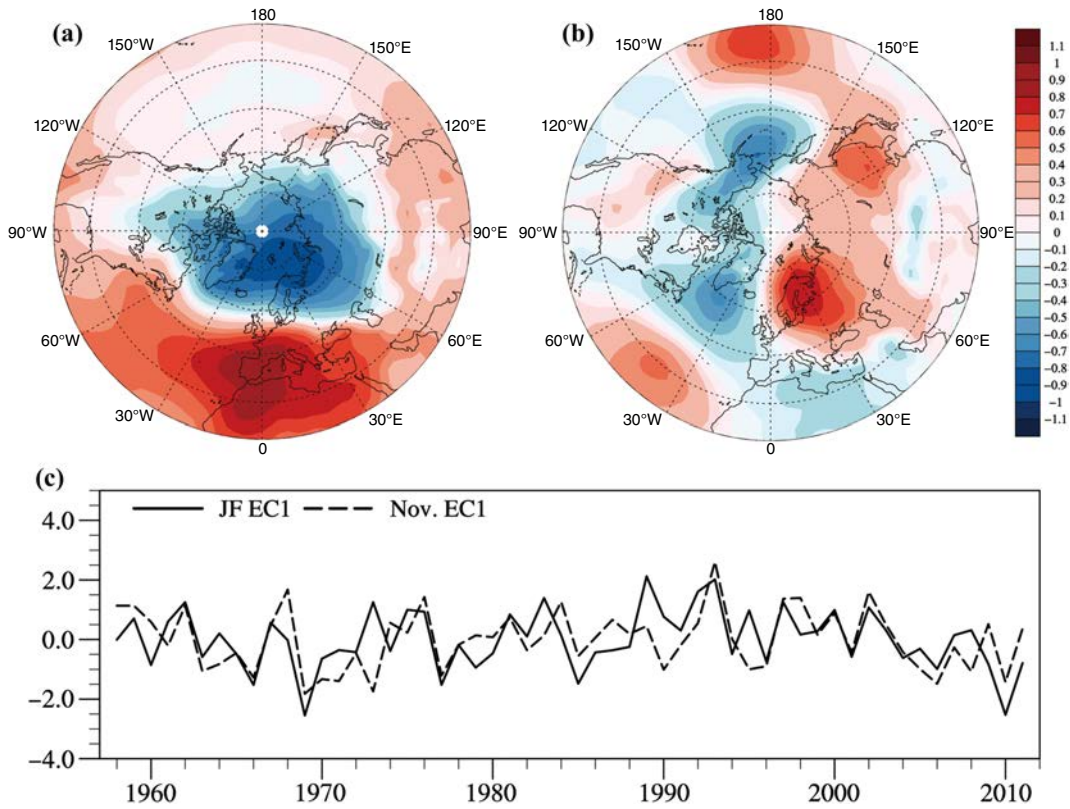


Figure 2. Spatial patterns of the first coupled SVD modes of January–February. SLP (a) and November SLP (b); time series of the expansion coefficients (c).

fraction of the explained variance is comparable with the 22% fraction of the NDJFMA SLP total variance explained by the AO mode of Thompson and Wallace (1998). The leading PCA pattern (Figure 3) bears a strong resemblance with the seesaw structure obtained in the previous experiments (Figures 1(a) and 2(b)), with correlation coefficients between the series of the leading November SLP principal component (PC1) and November CI and EC1 being 0.88 and 0.82, respectively.

The second PCA mode with an explained variance of 14.0% resembles the AO mode. The correlation coefficient between the series of the November SLP PC2 and the November AO index is 0.80, which corresponds to the finding of Ogi *et al.* (2004b) that the AO is not a leading mode of circulation variability in November.

The quantitative assessments of the complex relationships associated with the impact of the JF AO on the November SLP anomalies are summarized in Table 1. Most of the correlation coefficients are significant at the 99% level of confidence, and the significance of the few remaining coefficients exceeds the 90% level of confidence. This confirms the high confidence of the obtained results and conclusions.

These statistical results support the conclusion that the JF AO impacts November circulation, with the positive JF AO polarity inducing the dominance of the positive (negative) SLP anomalies in the Eastern (Western) Hemisphere in the middle and high latitudes of the Northern Hemisphere. In Novembers following winters of the

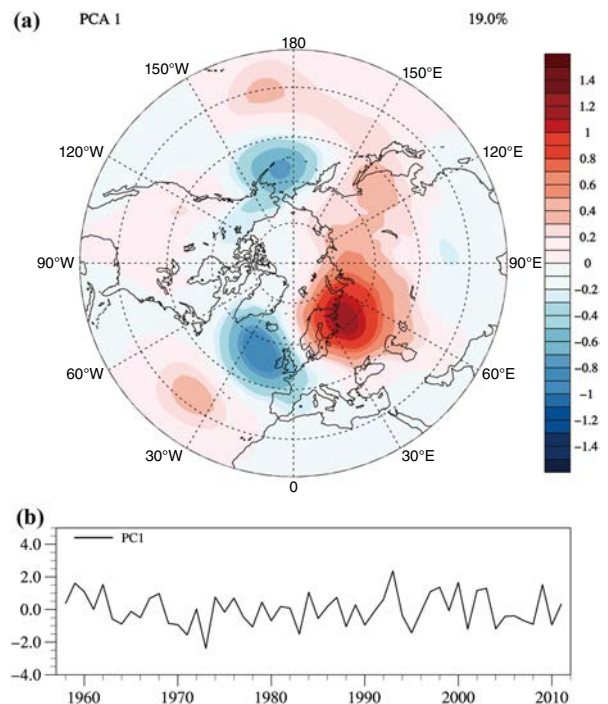


Figure 3. Leading PCA pattern of the November SLP anomalies north of 20°N (a) and time series of the November SLP PC1 (b).

negative AO polarity, the sign of the anomalies is reversed. The pattern of the November SLP variability associated with the preceding JF AO closely resembles the leading mode of the November SLP variability derived by the

Table 1. Correlation coefficients between the JF AO index (JF AO), expansion coefficients of the first coupled SVD modes of JF SLP (JF EC1) and November SLP (November EC1), circulation indices (CI) based on JF SLP (JF CI) and November SLP (November CI) and the PC1 of November SLP (November PC1) for the period from 1958 to 2011.

	JF EC1	JF CI	November PC1	November EC1	November CI
JF AO	0.87**	0.95**	0.27	0.38**	0.49**
JF EC1		0.97**	0.29*	0.54**	0.55**
JF CI			0.29*	0.48**	0.55**
November PC1				0.82**	0.88**
November EC1					0.93**

*Significant at the 5% level, **Significant at the 1% level.

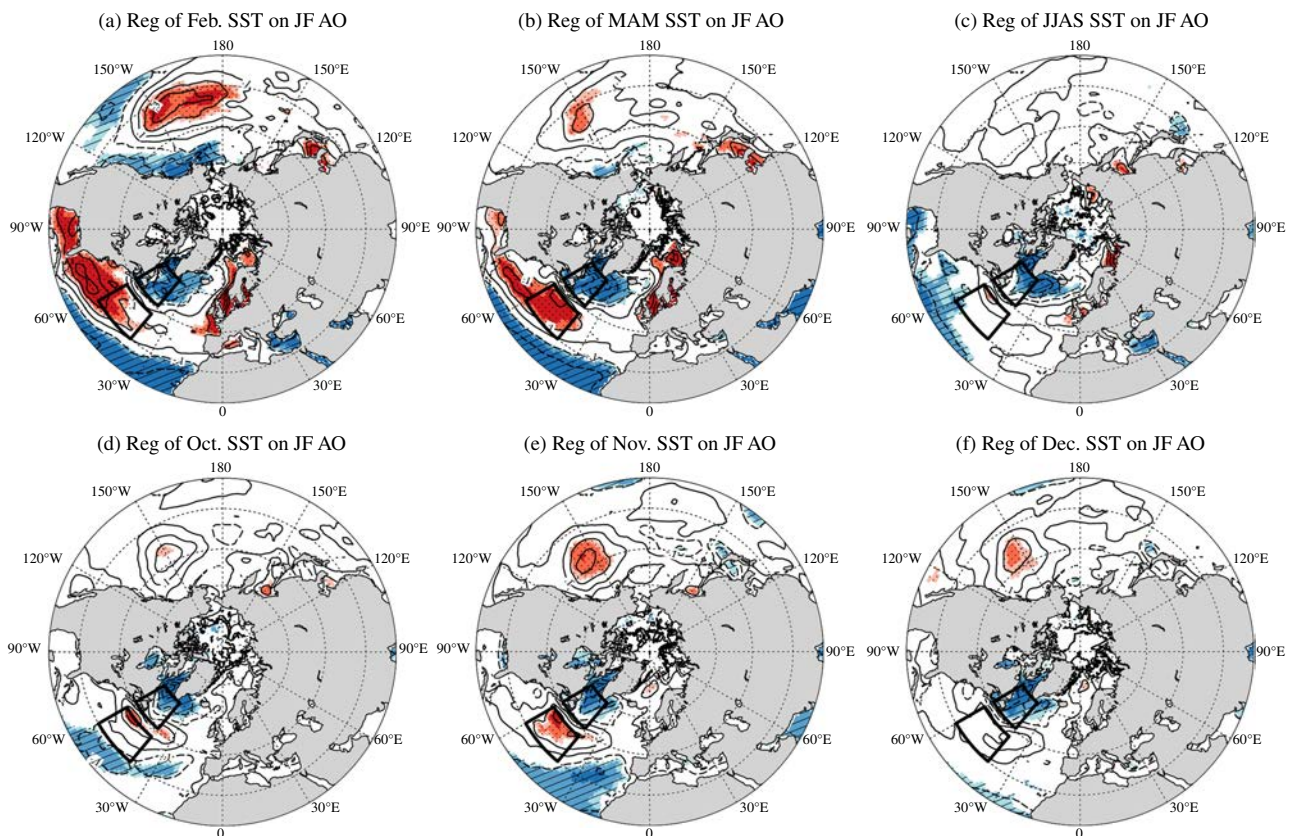


Figure 4. Lag regressions on the normalized JF AO index of SST monthly/seasonal mean values of February (a), MAM (b), JJAS (c), October (d), November (e) and December (f). Unit: $\text{K}(\text{SD})^{-1}$ (contours). Light, medium and heavy colour shadings indicate the areas where regression coefficients are significant at the 90, 95 and 99% confidence levels, respectively. The stipples (crosshatch) defines positive (negative) values.

PCA. The November seesaw mode could play an important role in affecting the variability of temperature over Northern Eurasia, as described by Kryzhov (2008), who linked this variability with the preceding wintertime AO.

4. Discussion of the mechanisms

The hemispheric-scale response of November circulation to the preceding JF AO is a new finding of the present study and the mechanisms of this 9-month lag response have not yet been studied. We suggest that this mechanism resides in the November re-emergence of the wintertime SST anomaly excited by the impact of the wintertime AO and an influence of the re-emerged SST anomaly on November circulation. To examine the impact of the preceding wintertime AO on SST with different lags, the

maps of SST regressed on the JF AO have been computed (Figure 4).

The strongest response of SST to the wintertime AO is markedly seen in the North Atlantic. In February, JF AO gives rise to surface cooling in the vicinity of the Labrador Sea through the enhanced wind speed, cold advection from higher latitudes and enhanced sensible and latent heat fluxes from the ocean to atmosphere. The significant cold anomaly centred over the Labrador Sea (northern box) persists from February through next December. Meanwhile, a significant warm anomaly over the western North Atlantic (southern box) persists only from February through May, after which it weakens and disappears during the June–September summer season (with the exclusion of the northernmost small area of the box). However, the positive SST anomaly over the southern box strengthens

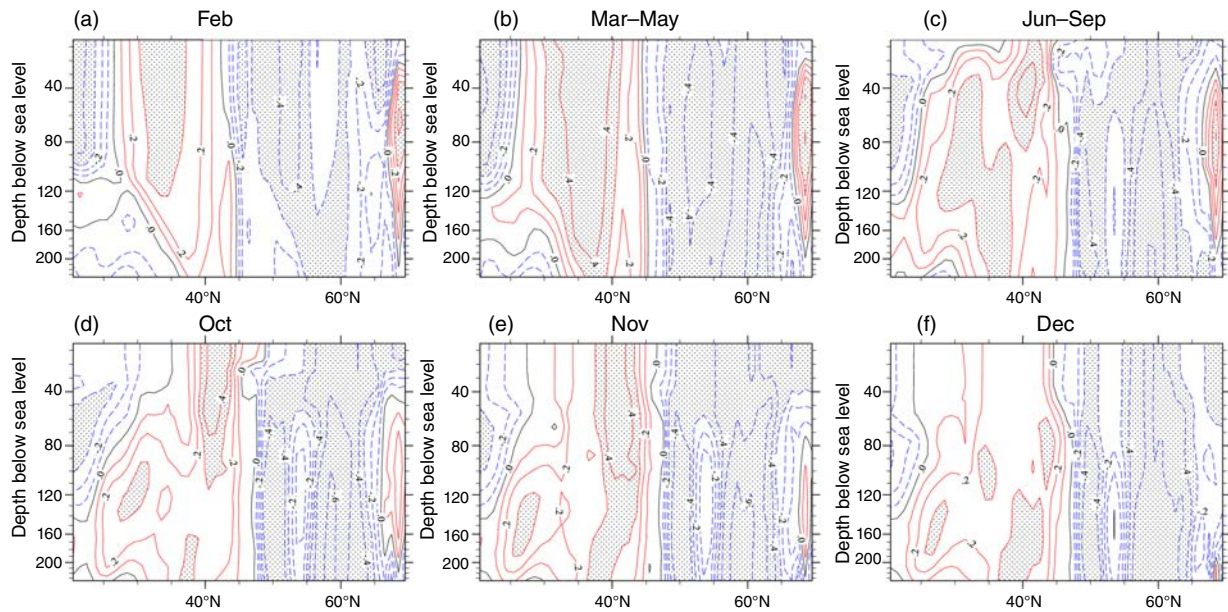


Figure 5. Cross-section from 20° to 70° N of the lag correlations between the JF AO index and monthly/seasonal mean values of water temperature in the upper 200 m layer of the ocean averaged over the belt 60° to 40° W of February (a), MAM (b), JJAS (c), October (d), November (e) and December (f). The grey shading indicates the area where correlation coefficients are significant at the 95% confidence level.

in October, reaches its maximum in November and disappears in December. Evolution of the SST anomaly in the southern box closely matches descriptions of the North Atlantic SST anomaly re-emergence given by Alexander and Deser (1995). The persistence of the SST anomaly in the Labrador Sea (northern box) is attributed to lower solar irradiance and stronger surface winds, which prevent the formation of the shallow surface mixed layer. Both wintertime and re-emerged November SST anomaly dipole patterns caused by the wintertime AO closely resemble the northern two-pole part of the North Atlantic tripole associated with the NAO (Mosdale and Timothy, 2006; Pan, 2007), which is expectable as it accounts for the close relationships between the wintertime AO and NAO.

The re-emergence of the positive SST anomaly is supported by the sequential evolution of subsurface water temperature anomalies. The cross-section from 20° to 70° N of the correlations between water temperature in the upper 200 m layer of the ocean averaged over the belt 60° – 40° W and the JF AO index is shown in Figure 5. The positive subsurface temperature anomaly over the western North Atlantic (30° – 42° N, 60° – 40° W), associated with the positive JF AO polarity, is prominent in February and persists through the MAM season. During the JJAS season, this positive signal is much weakened in the near surface layer (0–30 m) as the influence of net surface heat flux anomalies (increase of the solar irradiance and decrease of the turbulent fluxes from the ocean to atmosphere) strengthens and a shallow surface warm mixed layer forms, which masks the underlying anomalies. However, autumn storms destroy this shallow mixed layer and the warm anomalies maintained in the depth re-emerge to the surface in the western North Atlantic (southern box), peaking in November and being destroyed by the winter storms in December. These results (Figures 4 and 5) explain why the strongest

influence of the JF AO on the autumn circulation is confined to November, although the significant cold anomaly over the Labrador Sea (northern box) persists through December. Thus, the main November response of the North Atlantic SST to the preceding wintertime AO is the re-emerged northern two-pole part of the North Atlantic SST tripole pattern and associated increase (decrease) of the meridional SST gradient in the western part of the North Atlantic after the winters of the positive (negative) AO polarity.

These oceanic data analysis (Figures 4 and 5) is confirmed with analysis of other available data sets (HadISST, ERSST v2, ECDA v3.1 and SODA v2.2.4). The maps of SST (HadISST, ERSST v2) regressed on the JF AO (Figures S1 and S2, Supporting Information) were similar to our results (Figure 4). The sequential evolution of subsurface water temperature anomalies (ECDA v3.1 and SODA v2.2.4) shown in Figures S3 and S4 bears a strong resemblance with our result (Figure 5). The similarity of these results supports our belief that the ocean analysis dataset that we used is reliable.

To support this result, similar regression analysis has been applied through reverse succession. Figure 6 shows the regression of SST anomalies (February, MAM, October and November) on the following November CI and SLP PC1. Both indices indicate North Atlantic SST anomalies in February and spring (Figure 6(a), (b), (e), and (f)), similar to those associated with the impact of the JF AO shown in Figure 4. There are no significant SST anomalies in June–September when the wintertime SST anomalies are masked by the summer shallow surface mixed layer (not shown). Wintertime SST anomalies start to re-emerge in October and become strong in November (Figure 6(c), (d), (g), and (h)). Thus, the November seesaw phase following the positive polarity of the wintertime

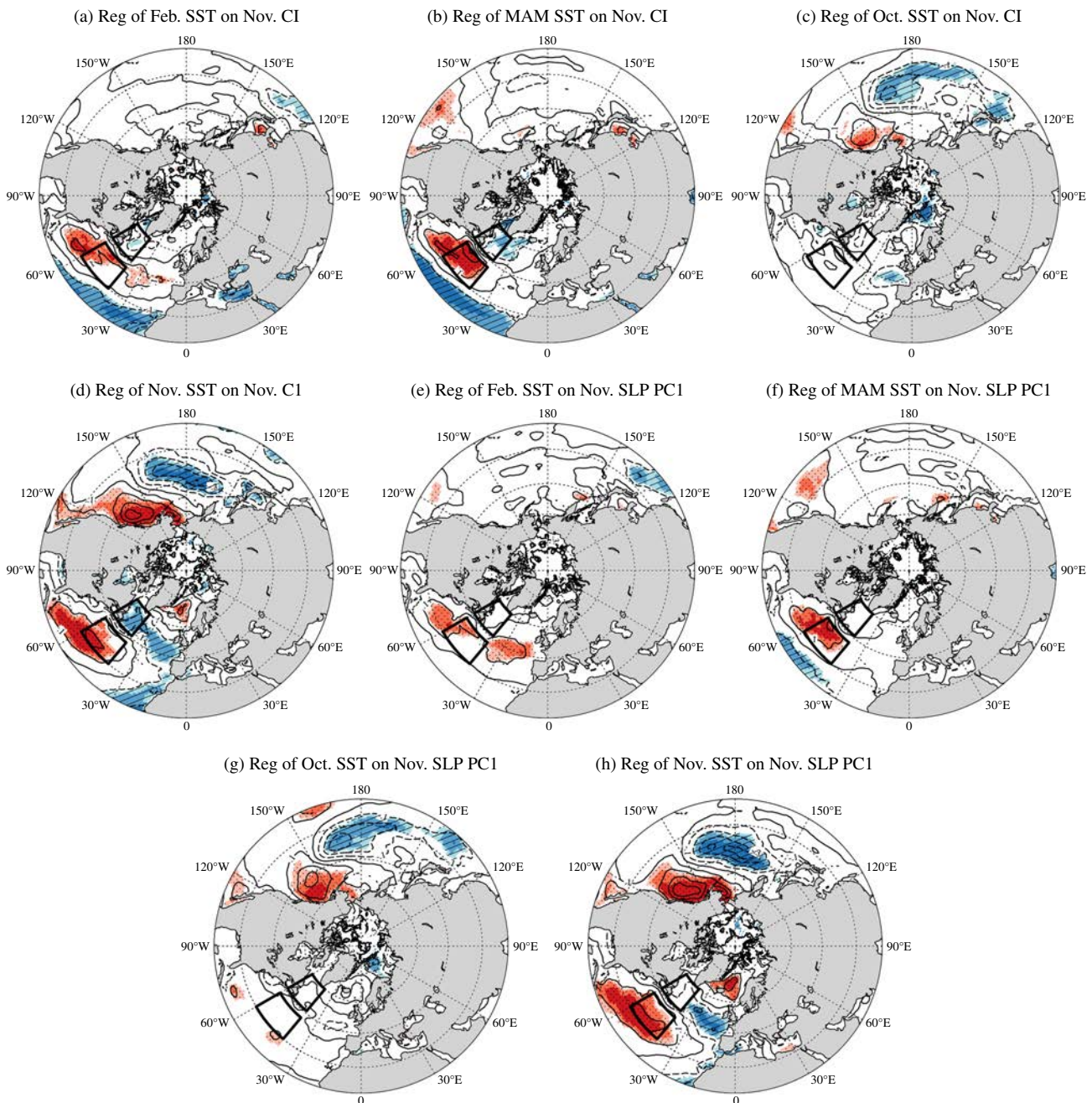


Figure 6. Regression of February (a, e), MAM (b, f), October (c, g) and November (d, h) SST on the November CI (upper) and PC1 (bottom). Unit: $K(SD)^{-1}$. Areas of light, medium and heavy colour shadings indicate the areas where regression coefficients are significant at the 90, 95 and 99 confidence levels, respectively. The stipples (crosshatch) defines positive (negative) values.

AO (Figures 1–3) is preceded by evolution of the North Atlantic SST anomalies closely resembling that forced by the positive polarity wintertime AO and resulting in the enhanced meridional SST gradient in the Western North Atlantic in November. This supports the hypothesis that re-emergence of the SST anomaly is one of the ways in which the wintertime AO signal is transmitted into autumn.

The mechanism of the Western North Atlantic SST gradient impact on circulation is discussed by Serreze *et al.* (2001). A climatological meridional gradient in SST is associated with the temperature contrast between the

warm northward-flowing North Atlantic Drift current and the cold southward flowing East Greenland current. It is known to affect the frontal activity in the vicinity of Greenland. This meridional SST gradient in a given area tends to drive baroclinic instability and, as discussed below, displacement of the upper troposphere jet stream, with both exciting cyclogenesis. Enhancement (weakening) of the SST gradient in November following winters of the positive (negative) AO polarity enhances (weakens) cyclogenesis in the area of the Icelandic low. That is, re-emergence of the SST anomaly, associated with preceding positive (negative) JF AO polarity, induces the formation of the

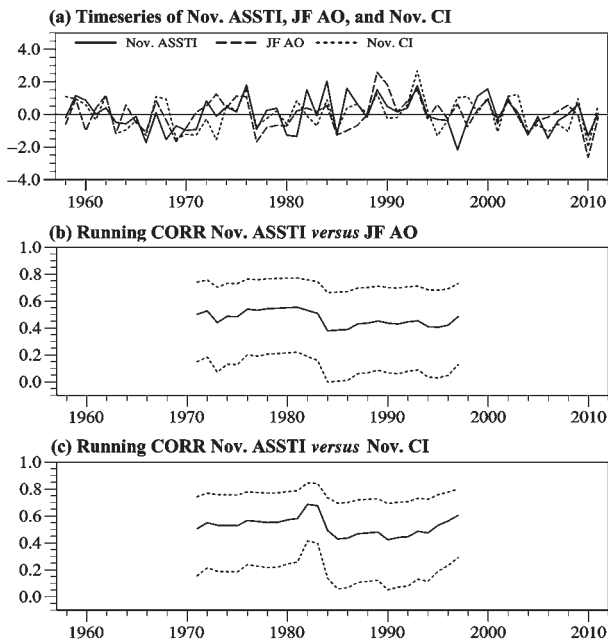


Figure 7. Normalized time series of the November ASSTI (solid), JF AO (long dash), November CI (short dash) (a); running correlations (solid) calculated over 27-year windows (plotted in the central year of the 27-year period) between November ASSTI and JF AO (b), November ASSTI and November CI (c) and their 95% confidence intervals (dashed).

November negative (positive) SLP anomaly over the western North Atlantic with associated enhancement (weakening) of warm advection into the eastern Arctic.

To quantitatively describe interannual variations of the northwestern Atlantic SST anomalies associated with preceding JF AO, we have constructed an index characterizing the November Atlantic SST meridional gradient (November ASSTI) as a difference of the SST anomalies averaged over the southern and northern boxes (Figure 7(a)). The JF AO index (JF CI) and November CI significantly correlate with the November ASSTI with coefficients of 0.51 (0.49) and 0.55, respectively (Table 2), with the correlations being stable in time (Figure 7(b) and (c)). Most of the correlation coefficients are significant at the 99% level of confidence. This confirms the high confidence of the obtained results and conclusions.

The confirmation that November ASSTI links the JF AO and November seesaw mode comes from the regression maps shown in Figure 8, which closely resemble those of Figures 1 and 2. Regression of JF SLP on the November ASSTI (Figure 8(a)) reveals a pattern resembling that of the AO, while regression of the November SLP on the November ASSTI (Figure 8(b)) reveals a pattern of the November SLP response to the wintertime AO, that is, the seesaw over the high and middle latitudes of the Northern Hemisphere characterized by the cyclonic anomalies in the western hemisphere from the North Pacific through the western North Atlantic and the anti-cyclonic anomalies extending from the West Europe through the East Asia. These results support the hypothesis that the re-emergence

of the North Atlantic SST anomalies links the wintertime AO and the November seesaw mode.

Intuitively, one may expect a link through the re-emergence of the North Pacific SST anomalies similar to that of the North Atlantic. Indeed, following the winters of the positive AO polarity, a warm anomaly in the Northeastern Pacific re-emerges in October and reaches its maximum in November. This anomaly increases a meridional SST gradient in the Aleutian low area and is favourable for enhancement of the Aleutian low. However, results for the North Pacific have a low statistical significance because the November pattern of the North Pacific SST anomalies associated with the positive November CI and SLP PC1 is a response of SST to the already enhanced Aleutian low, rather than the pattern which forces this enhancement. Additionally, the Aleutian low is within the area of the negative SLP anomalies (Figures 1(a), 2(b), 3, and 8(b)) corresponding to the positive November CI and SLP PC1. Possible explanations include the relationships between the Aleutian low with the El-Nino-Southern Oscillation (ENSO) phenomenon (Bjerknes, 1969), a biennial component in the ENSO variability (Rasmusson *et al.*, 1990), a tendency of the wintertime AO to be negative (positive) during the El-Nino (La-Nina) winters (e.g. Fletcher and Kushner, 2011) and a proposal by Nakamura *et al.* (2006, 2007) for the tendency of the positive (negative) wintertime AO to be followed by the development of El-Nino (La-Nina) in the next autumn.

The response of November Atlantic climate variability to the November ASSTI, shown in Figure 9, explains the mechanisms of the re-emerged SST anomaly impact on November circulation. After winters of the positive AO polarity, the increased meridional SST gradient over the western North Pacific drives upper-level positive zonal wind anomalies, implying a northward displacement of jet stream through the thermal wind relationship. Poleward displacement of jet stream induces the upward synoptic scale vertical motion over the northern part of jet stream exit region (Holton, 2004), which in turn enhances the convective activity (indicated by enhanced precipitation in Figure 9) in the area of Icelandic low where the Arctic frontal zone is located. The associated diabatic heating and enhancement of warm advection, caused by the deepened Icelandic low, give rise to the positive lower troposphere thickness anomaly in the vicinity of Greenland Sea, which reinforces the surface pressure to decrease (Holton, 2004). This strong coupling among diabatic heating, warm advection and positive lower troposphere thickness anomaly leads to a persistent low level cyclonic flow, which indicates that the cyclones from the Icelandic low propagate northward along the eastern Greenland coast rather than eastward along the Siberian coast, due to warm injection in the western North Pacific, and which results in the positive SLP anomalies over North Eurasia. After winters of negative AO polarity, the signs of impacts and anomalies are inverted.

Along with regression analysis we have performed a case study of the evolution of climatic anomalies followed the extremely positive JF AO of 1989 and extremely negative

Table 2. Correlation coefficients of the index of the November Atlantic Sea Surface Temperature (November ASSTI) with the January–February. AO index (JF AO), expansion coefficients of January–February. SLP (JF EC1) and November SLP (November EC1), circulation indices (CI) of January–February. SLP (JF CI) and November SLP (November CI) and the PC1 of November SLP (November PC1) for the period from 1958 to 2011.

	JF AO	JF EC1	JF CI	November PC1	November EC1	November CI
November ASSTI	0.51**	0.42**	0.49**	0.46**	0.44**	0.55**

*Significant at the 5% level, **Significant at the 1% level.

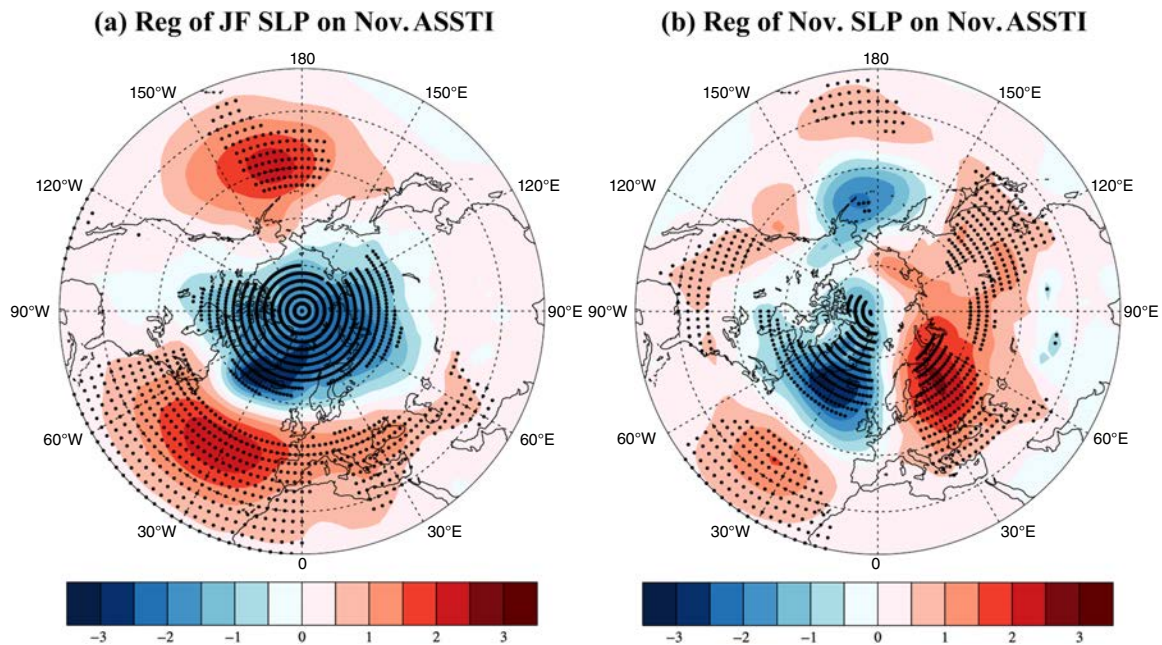


Figure 8. Regression of the JF (a) and November (b) SLP anomalies on the November ASSTI. Units: $\text{hPa}(\text{SD})^{-1}$. The dots indicate the area where regression coefficients are significant at the 95% confidence level.

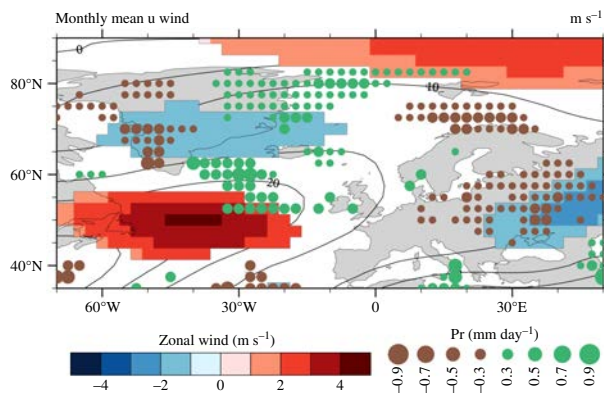


Figure 9. Regressions of November zonal wind at 200 hpa (shading) and precipitation (dot) on the November ASSTI. Contour denotes the November climatological zonal wind at 200 hpa. Only the values significant at the 90% confidence level or higher are shown.

JF AO of 2010. The sequential evolution of the wintertime SST anomalies over the western North Atlantic after the winters of extremes in the JF AO closely resembles and supports the results from regression analysis (Figure S5). The 9-month lag response of November circulation (Figure S6) also closely resembles that obtained in linear analysis and supports its results.

5. Conclusion

This study has demonstrated the influence of the wintertime AO on the following November circulation. On one hand, it has supported the results from the previous studies showing such influence in the Atlantic-European sector. On the other hand, it has yielded new findings. Particularly, this study has demonstrated that the November circulation response to the preceding wintertime AO operates on a hemispheric scale and closely resembles the leading EOF of November SLP. Another new finding is the evidence that the re-emergence of SST in the North Atlantic is a key component of the mechanism of the 9-month lag response of November circulation to the preceding wintertime AO.

Several statistical methods are used to show that winters of the positive (negative) AO polarity tend to be followed by positive (negative) SLP anomalies over North Eurasia and negative (positive) SLP anomalies over a large region from the Bering Sea through the North Atlantic. That is, the response of November SLP to the JF AO is a seesaw pattern in the middle and high latitudes with SLP anomalies of one sign spanning the Eastern Hemisphere and SLP anomalies of the opposite sign spanning the Western Hemisphere. This seesaw pattern closely resembles the leading hemispheric-scale EOF of November SLP, which explains 19% of its total variability, with the correlation

coefficient between the series of the November CI, corresponding to the seesaw pattern, and the first principal component of November SLP, being 0.87.

The key distinctive mechanisms of the 9-month lag in the November circulation response to the preceding wintertime AO is caused by the re-emergence of the wintertime SST anomalies over the western North Atlantic. The negative SST anomaly over the northwestern North Atlantic, caused by the preceding JF AO positive polarity, persists through December, whereas the positive SST anomaly, also caused by the preceding JF AO positive polarity, re-emerges due to the enhancing autumn storm activity and reaches its maximum in November.

This enhanced meridional SST gradient induces baroclinicity and displacement of the upper troposphere jet stream, with both exciting cyclogenesis in November. That is, the re-emergence of SST causes the negative November SLP anomaly over the North Atlantic associated with the enhanced cyclonic activity in the Arctic frontal zone and provides an enhanced warm advection to the eastern Arctic with the corresponding changes in the hemispheric circulation.

Our statistical study has provided evidence of the relationships between November circulation and the preceding wintertime AO, and we have proposed physically plausible mechanisms to explain the revealed relationships. However, a statistical study cannot produce physical evidence in support of statistical relationships. Therefore, we plan to clarify the mechanisms of the revealed relationships with model experiments.

Acknowledgements

This work was carried out with the support of the Korea Meteorological Administration Research and Development Program under Grant KMIPA 2015-2081 and the Rural Development Administration Cooperative Research Program for Agriculture Science and Technology Development under Grant Project No. PJ009953, Republic of Korea.

Supporting Information

The following supporting information is available as part of the online article:

Figure S1. Lag regressions on the normalized JF AO index of SST (HadISST) monthly/seasonal mean values of February (a), MAM (b), JJAS (c), October (d), November (e) and December (f) for the period 1958–2011. Unit: $K(SD)^{-1}$ (contours). Light, medium and heavy colour shadings indicate the areas where regression coefficients are significant at the 90, 95 and 99% confidence levels, respectively.

Figure S2. Lag regressions on the normalized JF AO index of SST (ERSST v2) monthly/seasonal mean values of February (a), MAM (b), JJAS (c), October (d), November (e) and December (f) for the period 1958–2008. Unit: $K(SD)^{-1}$ (contours). Light, medium and heavy colour

shadings indicate the areas where regression coefficients are significant at the 90, 95 and 99% confidence levels, respectively.

Figure S3. Cross-section from 20° to 70°N of the lag correlations between the JF AO index and monthly/seasonal mean values of water temperature (ECDA v3.1) in the upper 200 m layer of the ocean averaged over the belt 60°–40°W of February (a), MAM (b), JJAS (c), October (d), November (e) and December (f) for the period 1961–2010. The grey shading indicates the area where correlation coefficients are significant at the 95% confidence level.

Figure S4. Cross-section from 20° to 70°N of the lag correlations between the JF AO index and monthly/seasonal mean values of water temperature (SODA v2.2.4) in the upper 200 m layer of the ocean averaged over the belt 60°–40°W of February (a), MAM (b), JJAS (c), October (d), November (e) and December (f) for the period 1958–2010. The grey shading indicates the area where correlation coefficients are significant at the 95% confidence level.

Figure S5. Composites of monthly SST (HadISST) anomalies of February (a, d, g), July (b, e, h) and November (c, f, i) for the extreme positive JF AO (top; 1989), negative JF AO (middle; 2010) and their difference (bottom).

Figure S6. SLP anomalies in the extreme positive (a), negative (b) JF AO cases and its difference (c).

References

- Alexander MA, Deser C. 1995. A mechanism for the recurrence of wintertime midlatitude SST anomalies. *J. Phys. Oceanogr.* **25**: 122–137, doi: 10.1175/1520-0485(1995)025<0122:AMFTRO>2.0.CO;2.
- Alexander MA, Deser C, Timlin MS. 1999. The reemergence of SST anomalies in the North Pacific Ocean. *J. Clim.* **12**: 2419–2433, doi: 10.1175/1520-0442(1999)012<2419:TROSAI>2.0.CO;2.
- Balmaseda MA, Mogensen K, Weaver AT. 2013a. Evaluation of the ECMWF Ocean reanalysis ORAS4. *Q. J. Roy. Meteorol. Soc.* **139**: 1132–1161, doi: 10.1002/qj.2063.
- Balmaseda MA, Trenberth KE, Källén E. 2013b. Distinctive climate signals in reanalysis of global ocean heat content. *Geophys. Res. Lett.* **40**: 1754–1759, doi: 10.1002/grl.50382.
- Bamzai AS. 2003. Relationship between snow cover variability and Arctic Oscillation index on a hierarchy of time scales. *Int. J. Climatol.* **23**: 131–142, doi: 10.1002/joc.854.
- Barriopedro D, García-Herrera R, Hernández E. 2006. The role of snow cover in the Northern Hemisphere winter to summer transition. *Geophys. Res. Lett.* **33**: L14708, doi: 10.1029/2006GL025763.
- Bjerknes J. 1969. Atmospheric teleconnections from the equatorial Pacific. *Mon. Weather Rev.* **97**: 163–172, doi: 10.1175/1520-0493(1969)097<0163:ATFTEP>2.3.CO;2.
- Bretherton CS, Smith C, Wallace JM. 1992. An intercomparison of methods for finding coupled patterns in climate data. *J. Clim.* **5**: 541–560, doi: 10.1175/1520-0442(1992)005<0541:AIOMFF>2.0.CO;2.
- Bretherton CS, Widmann M, Dymnikov VP, Wallace JM, Blade I. 1999. The effective number of spatial degrees of freedom of a time-varying field. *J. Clim.* **12**: 1990–2009, doi: 10.1175/1520-0442(1999)012<1990:TENOSD>2.0.CO;2.
- Carton JA, Giese BS. 2008. A reanalysis of ocean climate using simple ocean data assimilation (SODA). *Mon. Weather Rev.* **136**: 2999–3017, doi: 10.1175/2007MWR1978.1.
- Carton JA, Chepurin G, Cao X, Giese B. 2000. A simple ocean data assimilation analysis of the global upper ocean 1950–95. Part I: methodology. *J. Phys. Oceanogr.* **30**: 294–309, doi: 10.1175/1520-0485(2000)030<0294:ASODAA>2.0.CO;2.
- Chang YS, Zhang S, Rosati A, Delworth TL, Stern WF. 2013. An assessment of oceanic variability for 1960–2010 from the GFDL

- ensemble coupled data assimilation. *Clim. Dyn.* **40**(3–4): 775–803, doi: 10.1007/s00382-012-1412-2.
- Deser C, Alexander MA, Xie SP, Phillips AS. 2010. Sea surface temperature variability: patterns and mechanisms. *Annu. Rev. Mar. Sci.* **2**: 115–143, doi: 10.1146/annurev-marine-120408-151453.
- Fletcher CJ, Kushner PJ. 2011. The role of linear interference in the annular mode response to tropical SST forcing. *J. Clim.* **24**: 778–794, doi: 10.1175/2010JCLI3735.1.
- Gong DY, Wang SW, Zhu JH. 2001. East Asian winter monsoon and Arctic oscillation. *Geophys. Res. Lett.* **28**: 2073–2076, doi: 10.1029/2000GL012311.
- Hirahara S, Ishii M, Fukuda Y. 2014. Centennial-scale sea surface temperature analysis and its uncertainty. *J. Clim.* **27**: 57–75, doi: 10.1175/JCLI-D-12-00837.1.
- Holton JR. 2004. *An Introduction to Dynamic Meteorology*, 4th edn. Elsevier Academic Press: San Diego, CA.
- Ishii M, Shouji A, Sugimoto S, Matsumoto T. 2005. Objective analyses sea-surface temperature and marine meteorological variables for the 20th century using ICOADS and the Kobe Collection. *Int. J. Climatol.* **25**: 865–879, doi: 10.1002/joc.1169.
- Kalnay E, Kanamitsu M, Kistler R, Collins W, Deaven D, Derber J, Gandin L, Iredell M, Saha S, White G, Woollen J, Zhu Y, Chelliah M, Ebisuzaki W, Higgins W, Janowiak J, Mo KC, Ropelewski C, Wang J, Leetma A, Reynolds R, Jenne R, Joseph D. 1996. The NCEP/NCAR 40-year reanalysis project. *Bull. Am. Meteorol. Soc.* **77**: 437–471, doi: 10.1175/1520-0477(1996)077<0437:TNYRP>2.0.CO;2.
- Kryjov VN. 2002. The influence of the winter Arctic oscillation on the northern Russia spring temperature. *Int. J. Climatol.* **22**: 779–785, doi: 10.1002/joc.746.
- Kryjov VN. 2004. Searching for circulation patterns affecting Northern Europe annual temperature. *Atmos. Sci. Lett.* **5**: 23–34, doi: 10.1016/j.atmoscilet.2003.11.00.
- Kryzhov VN. 2008. Causes of November cooling of the 1980s–1990s in European Russia. *Russ. Meteorol. Hydrol.* **33**: 1–8, doi: 10.3103/S1068373908010019.
- Livezey RE, Chen WY. 1983. Statistical field significance and its determination by Monte Carlo techniques. *Mon. Weather Rev.* **111**: 46–59, doi: 10.1175/1520-0493(1983)111<0046:SFSASID>2.0.CO;2.
- Mosdala TJ, Timothy J. 2006. Granger causality of coupled climate processes: ocean feedback on the North Atlantic Oscillation. *J. Clim.* **19**: 1182–1194, doi: 10.1175/JCLI3653.1.
- Nakamura T, Tachibana Y, Honda M, Yamane S. 2006. Influence of the Northern Hemisphere annular mode on ENSO by modulating westerly wind bursts. *Geophys. Res. Lett.* **33**: L07709, doi: 10.1029/2005GL025432.
- Nakamura T, Tachibana Y, Shimoda H. 2007. Importance of cold and dry surges in substantiating the NAM and ENSO relationship. *Geophys. Res. Lett.* **34**: L22703, doi: 10.1029/2007GL031220.
- Namias J, Born RM. 1970. Temporal coherence in North Pacific sea-surface temperature patterns. *J. Geophys. Res.* **75**: 5952–5955, doi: 10.1029/JC075i030p05952.
- Namias J, Born RM. 1974. Further studies of temporal coherence in North Pacific sea surface temperatures. *J. Geophys. Res.* **79**: 797–398, doi: 10.1029/JC079i006p00797.
- North GR, Bell TL, Cahalan RF, Moeng FJ. 1982. Sampling errors in the estimation of empirical orthogonal functions. *Mon. Weather Rev.* **110**: 699–706, doi: 10.1175/1520-0493(1982)110<0699:SEITEO>2.0.CO;2.
- Ogi M, Tachibana Y, Yamazaki K. 2003a. Impact of the wintertime North Atlantic Oscillation (NAO) on the summertime atmospheric circulation. *Geophys. Res. Lett.* **30**: 1704, doi: 10.1029/2003GL017280.
- Ogi M, Yamazaki K, Tachibana Y. 2003b. Solar cycle modulation of the seasonal linkage of the North Atlantic Oscillation (NAO). *Geophys. Res. Lett.* **30**: 2170, doi: 10.1029/2003GL018545.
- Ogi M, Tachibana Y, Yamazaki K. 2004a. The connectivity of the winter North Atlantic Oscillation (NAO) and the summer Okhotsk High. *J. Meteorol. Soc. Jpn.* **82**: 905–913, doi: 10.2151/jmsj.2004.905.
- Ogi M, Yamazaki K, Tachibana Y. 2004b. The summertime annular mode in the Northern Hemisphere and its linkage to the winter mode. *J. Geophys. Res.* **109**: D20114, doi: 10.1029/2004JD004514.
- Pan LL. 2007. Synoptic eddy feedback and air–sea interaction in the North Atlantic region. *Clim. Dyn.* **29**: 6, doi: 10.1007/s00382-007-0256-7.
- Rasmusson EM, Wang X, Ropelewski CF. 1990. The biennial component of ENSO variability. *J. Mar. Syst.* **1**: 71–96, doi: 10.1016/0924-7963(90)90153-2.
- Rayner NA, Parker DE, Horton EB, Folland CK, Alexander LV, Rowell DP, Kent EC, Kaplan A. 2003. Global analyses of sea surface temperature, sea ice, and night marine air temperature since the late nineteenth century. *J. Geophys. Res.* **108**(D14): 4407, doi: 10.1029/2002JD002670.
- Rayner N, Kaplan A, Kent EC, Reynolds RW, Brohan P, Casey KS, Kennedy JJ, Woodruff SD, Smith TM, Donlon C, Breivik LA, Eastwood S, Ishii M, Brandon T. 2009. Evaluating climate variability and change from modern and historical SST observation. In *Proceedings of OceanObs '09: Sustained Ocean Observations and Information for Society*, Vol. 2, Hall J, Harrison DE, Stammer D (eds). ESA Publication WPP-306. Venice, Italy.
- Rigor IG, Wallace JM, Colony RL. 2002. On the response of sea ice to the Arctic Oscillation. *J. Clim.* **15**: 2648–2663, doi: 10.1175/1520-0442(2002)015<2648:ROSITT>2.0.CO;2.
- Serreze MC, Lynch AH, Clark MP. 2001. The Arctic frontal zone as seen in the NCEP-NCAR reanalysis. *J. Clim.* **14**: 1550–1567, doi: 10.1175/1520-0442(2001)014<1550:TAFZAS>2.0.CO;2.
- Smith TM, Reynolds RW. 2004. Improved extended reconstruction of SST (1854–1997). *J. Clim.* **17**: 2466–2477, doi: 10.1175/1520-0442(2004)017<2466:IEROS>2.0.CO;2.
- Thompson DWJ, Wallace JM. 1998. The Arctic Oscillation signature in the wintertime geopotential height and temperature fields. *Geophys. Res. Lett.* **25**: 1297–1300, doi: 10.1029/98GL00950.
- Thompson DWJ, Wallace JM. 2000. Annular modes in the extratropical circulation. Part I: month-to-month variability. *J. Clim.* **13**: 1000–1016, doi: 10.1175/1520-0442(2000)013<1000:AMITEC>2.0.CO;2.
- Thompson DWJ, Wallace JM, Hegerl GC. 2000. Annular modes in the extratropical circulation. Part II: trends. *J. Clim.* **13**: 1018–1036, doi: 10.1175/1520-0442(2000)013<1018:AMITEC>2.0.CO;2.
- Thomson, Wallace. 2000.
- Uppala SM, Källberg PW, Simmons AJ, Andrae U, da Costa Bechtold V, Fiorino M, Gibson JK, Haseler J, Hernandez A, Kelly GA, Li X, Onogi K, Saarinen S, Sokka N, Allan RP, Andersson E, Arpe K, Balmasada MA, Beljaars ACM, van de Berg L, Bidlot J, Bormann N, Caires S, Chevallier F, Dethof A, Dragosavac M, Fisher M, Fuentes M, Hagemann S, Hólm E, Hoskins BJ, Isaksen I, Janssen PAEM, Jenne R, McNally AP, Mahfouf J-F, Morcrette J-J, Rayner NA, Saunders RW, Simon P, Sterl A, Trenberth KE, Untch A, Vasiljevic D, Viterbo P, Woollen J. 2005. The ERA-40 re-analysis. *Q. J. R. Meteorol. Soc.* **131**: 2961–3012, doi: 10.1256/qj.04.176.
- Venegas SA, Mysak LA, Straub DN. 1997. Atmosphere-ocean coupled variability in the South Atlantic. *J. Clim.* **10**: 2904–2920, doi: 10.1175/1520-0442(1997)010<2904:AOCVIT>2.0.CO;2.
- Wallace JM, Jiang Q. 1987. On the observed structure of the interannual variability of the atmosphere/ocean climate system. In *Atmospheric and Oceanic Variability*, Cattle H (ed). Royal Meteorological Society, 17–43. Bracknell, Berkshire.
- Wang J, Zhang J, Watanabe E, Ikeda M, Mizobata K, Walsh JE, Bai X, Wu B. 2009. Is the dipole anomaly a major driver to record lows in Arctic summer sea ice extent? *Geophys. Res. Lett.* **36**: L05706, doi: 10.1029/2008GL036706.
- Wu B, Wang J, Walsh JE. 2006. Dipole anomaly in the winter Arctic atmosphere and its association with sea ice motion. *J. Clim.* **19**: 210–225, doi: 10.1175/JCLI3619.1.
- Yasunaka AS, Hanawa K. 2011. Intercomparison of historical sea surface temperature datasets. *Int. J. Climatol.* **31**: 1056–1073, doi: 10.1002/joc.2104.